



Center/Chair of
Materials Science
& Nanotechnologies

Առաջընթաց արդյունավետ գիտություն «ԱԱԳ-2026»

ՍԵՆՍՈՐԱՅԻՆ ՀԱՄԱԿԱՐԳԵՐԻ ՆԱԽԱԳԾՈՒՄ և ՊԱՏՐԱՍՏՈՒՄ ՆԱՆՈԿԱՌՈՒՅՎԱԾՔԱՅԻՆ ՆՅՈՒԹԵՐԻ ՀԻՄԱՆ ՎՐԱ

This research was funded by the Higher Education and Science Committee of MESCS RA (Research project N° 24LCG- 2J001)

International Journal of Smart and Nano Materials (Q1)

Ultra-high selective hydrogen peroxide vapor sensor based on the Fe₂O₃/MWCNTs nanocomposite

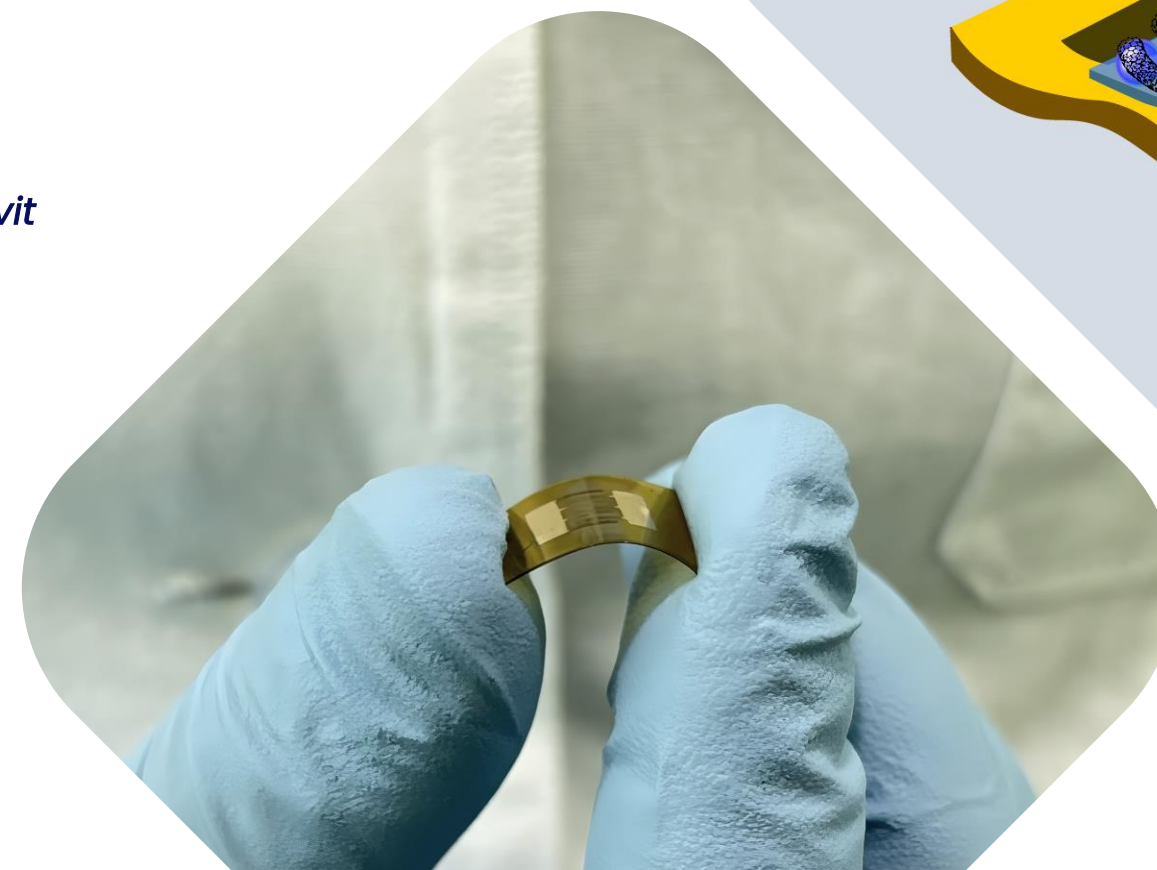
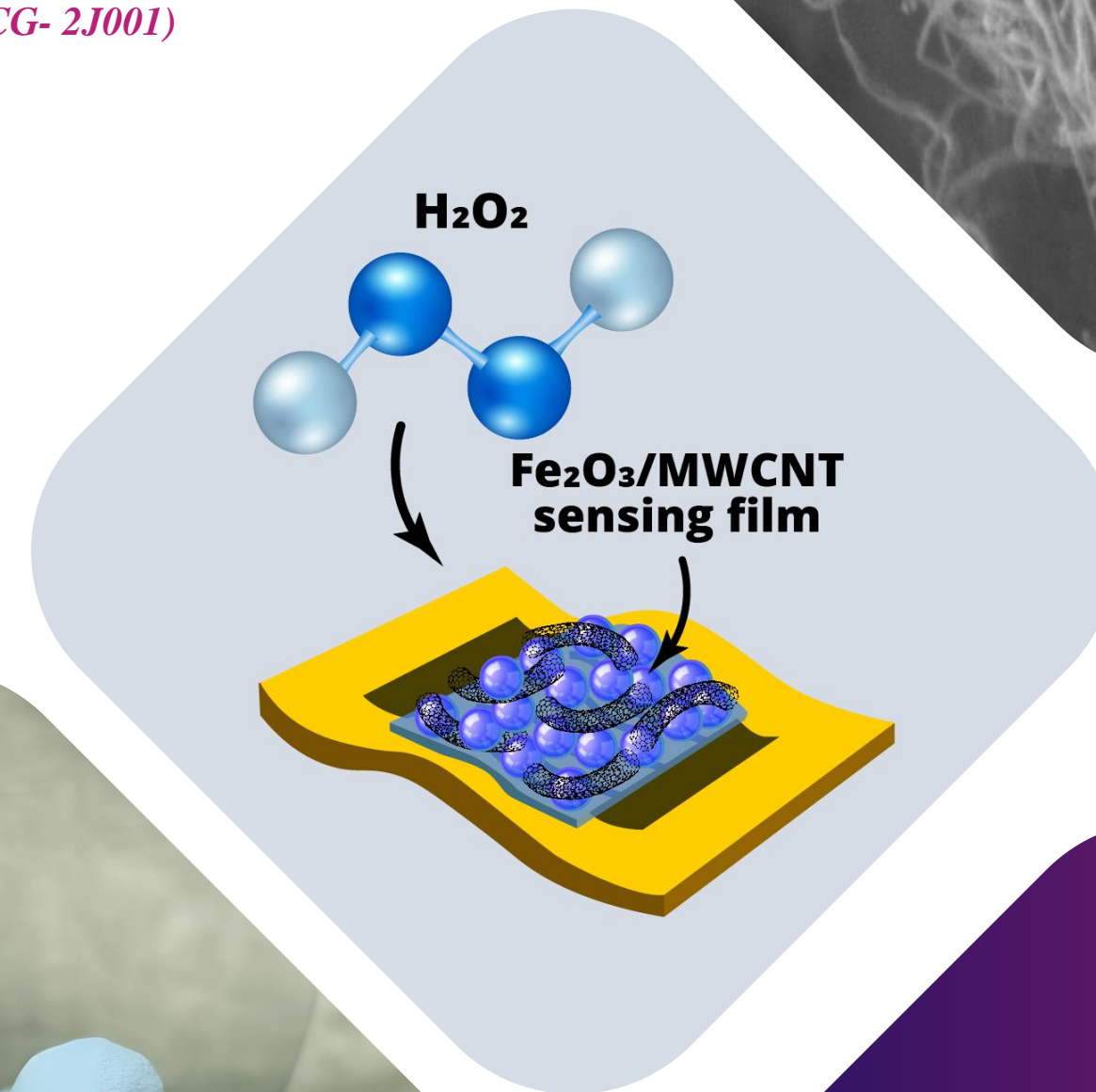
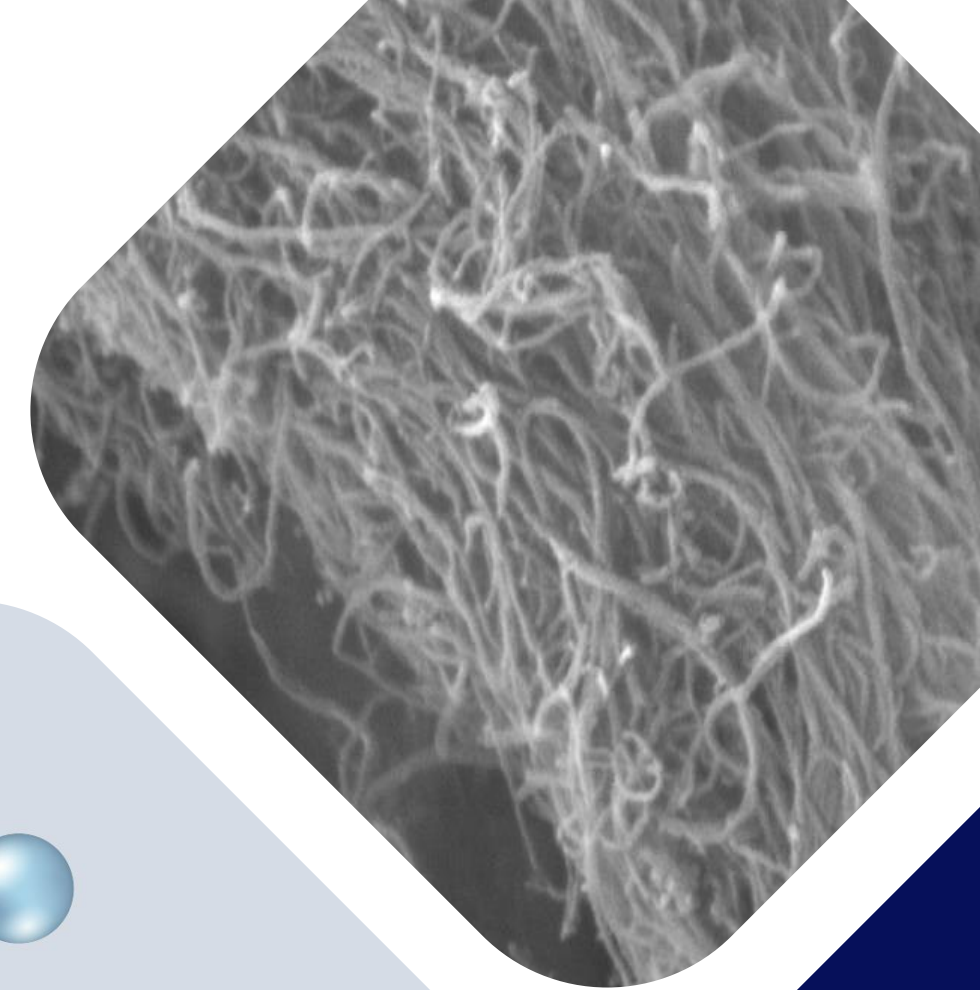
Artak Sayunts, Rima Papovyan, Gevorg Shahkhatuni, Zarine Simonyan, Davit

Kananov, Gabriel Gevorgyan, Dušan Kopecký & Mikayel Aleksanyan

Center of Materials Science and Nanotechnologies, Yerevan State University

Rima Papovyan

rimapapovyan@ysu.am



Gas sensor fabrication & testing

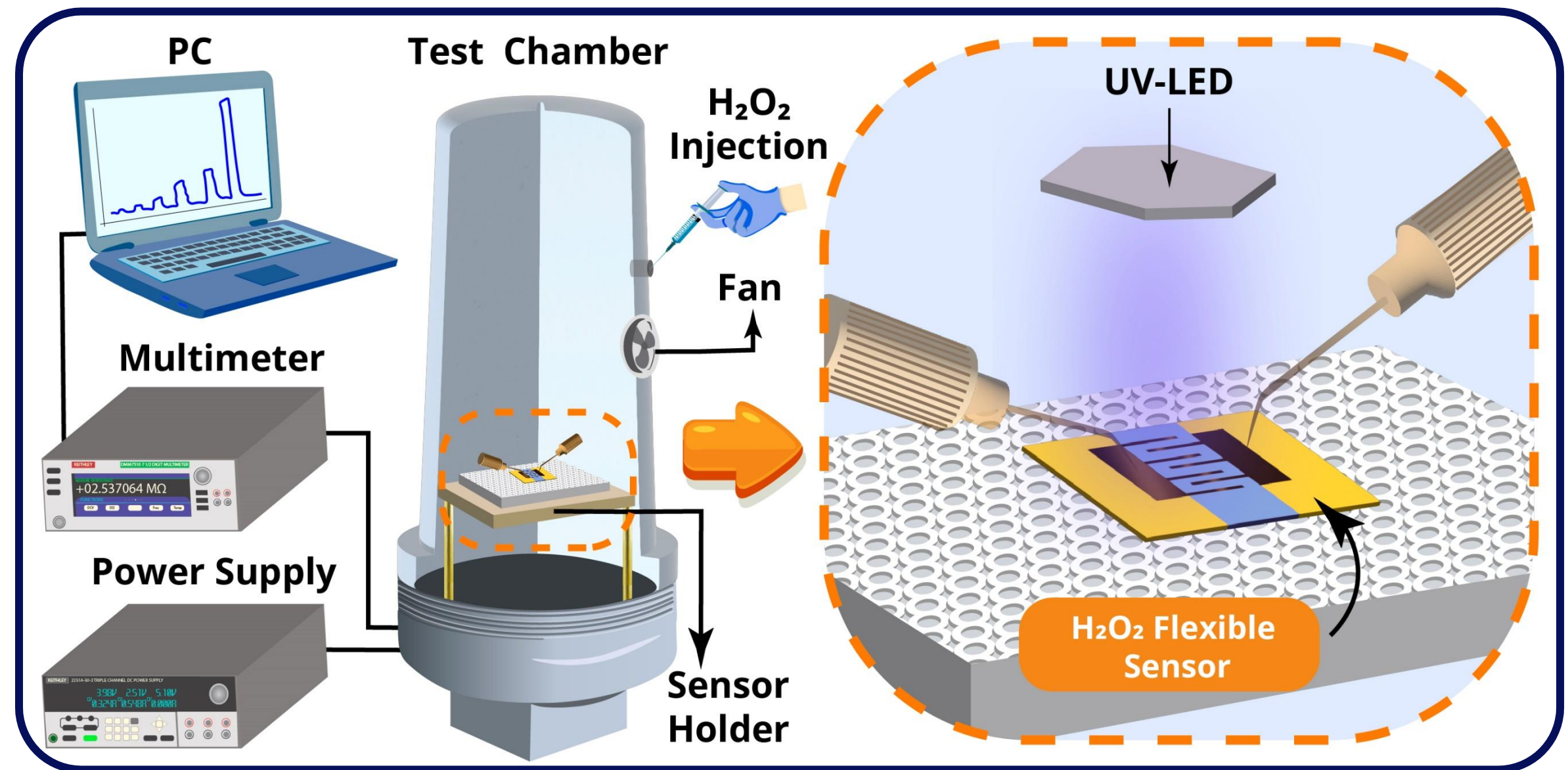
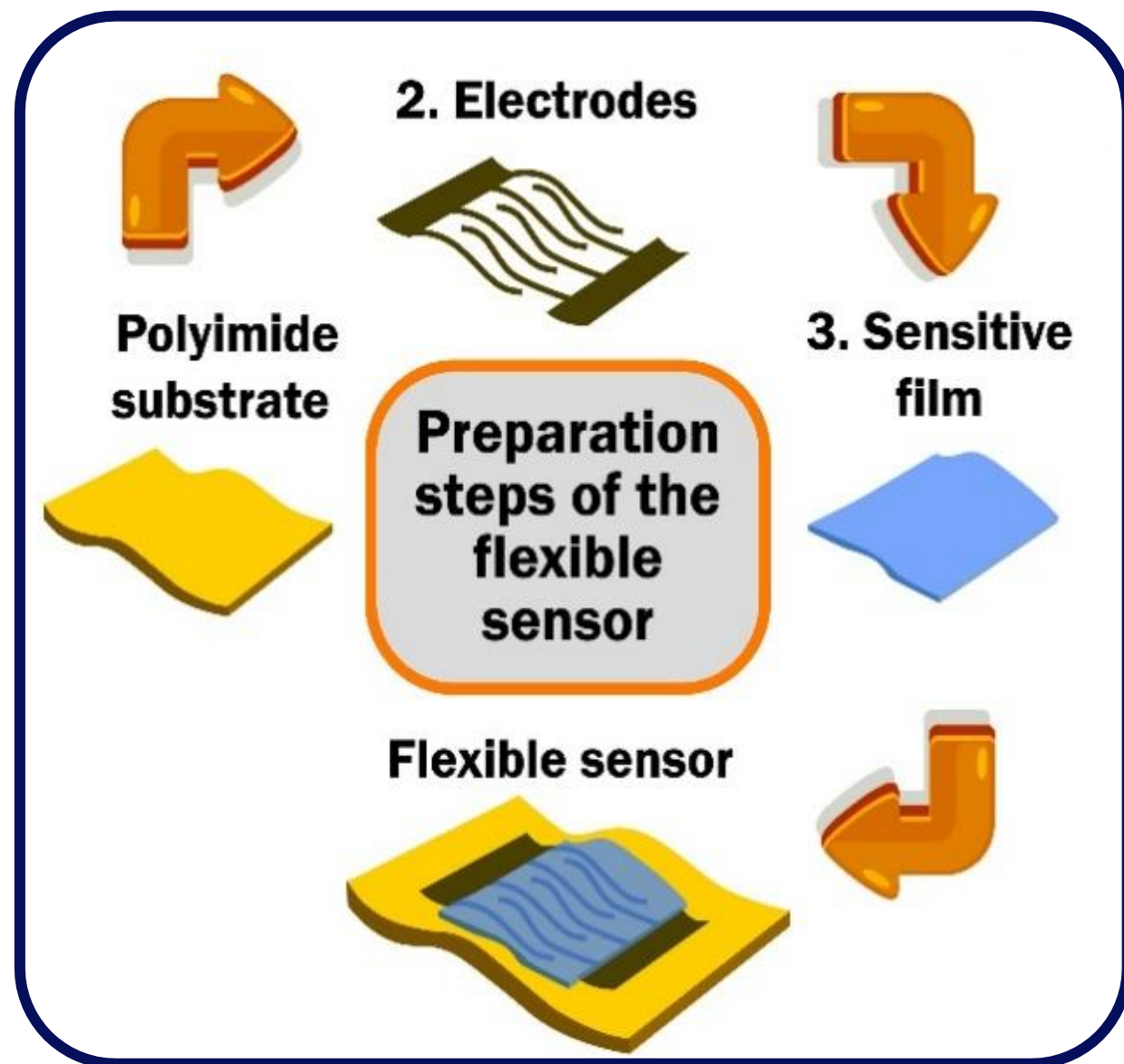


Figure 1. Schematic illustration of the flexible sensor preparation steps

Figure 2. Schematic illustration of the HPV sensor testing system

Characterization

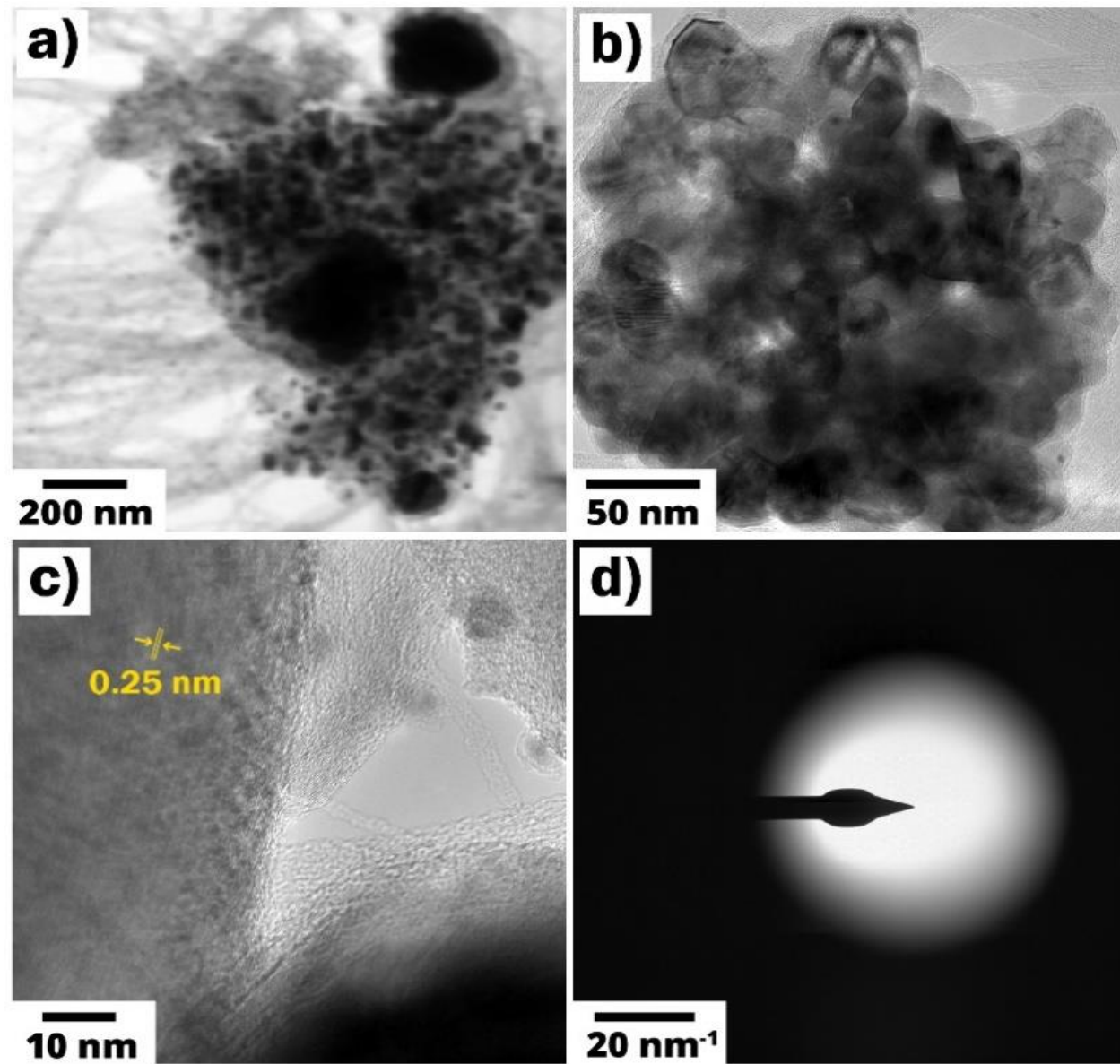


Figure 3. Low (a, b) and high-resolution (c) TEM images and SAED pattern (d) of the Fe_2O_3 material

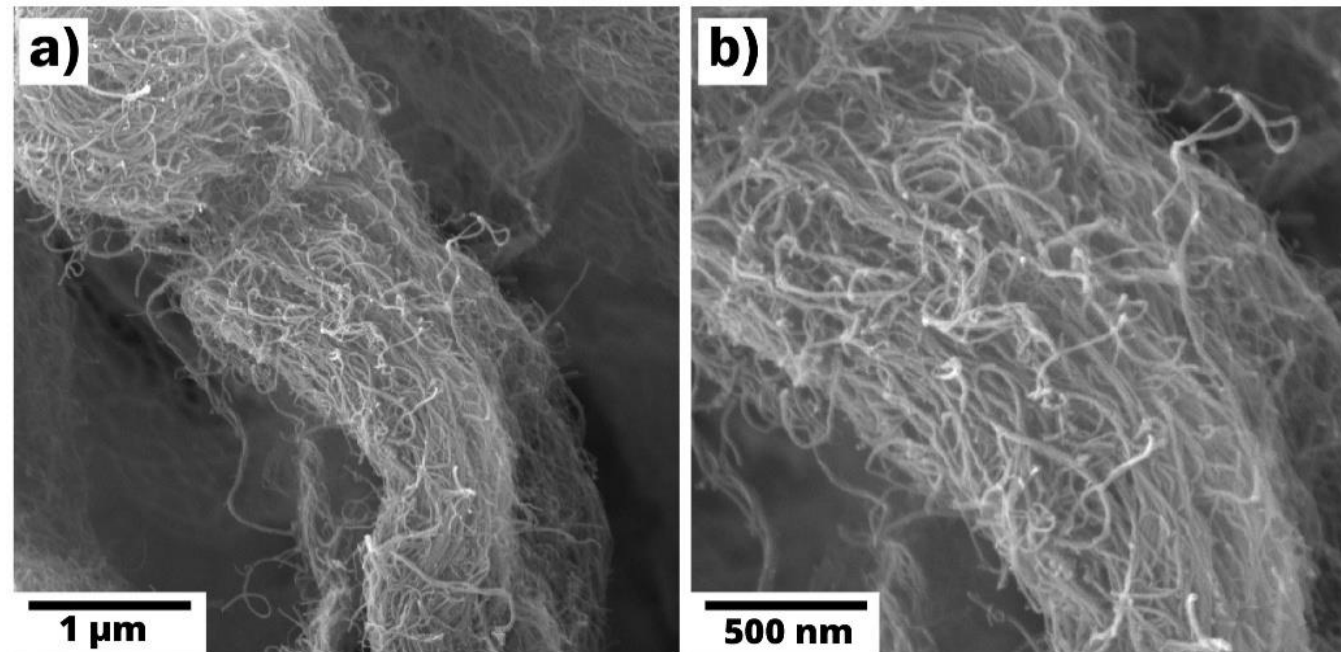


Figure 4. SEM images of the MWCNTs with the scalebars of $1 \mu m$ (a) and 500 nm (b).

SEM images showed that the MWCNTs formed interwoven networks with lengths of tens of micrometers and diameters of 10–20 nm. TEM analysis of the MWCNTs revealed a hexagonal crystal structure with a characteristic interlayer spacing of 0.34 nm.

TEM analysis confirmed the octahedral $\alpha\text{-}Fe_2O_3$ structure with grain sizes ranging from 25–40 nm and an interlayer spacing of approximately 0.25 nm. The SAED pattern revealed blurred diffraction rings, confirming the polycrystalline nature of the Fe_2O_3 material.

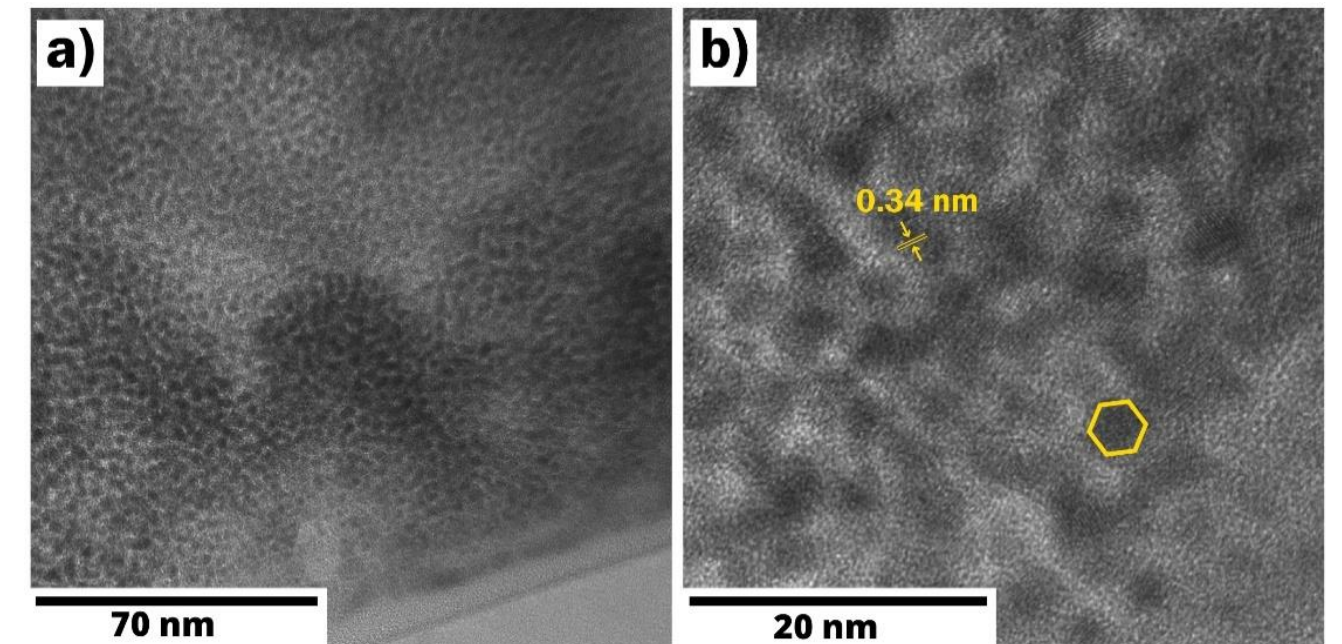


Figure 5. TEM images of the MWCNTs with the scalebars of 70 nm (a) and 20 nm (b).

Characterization

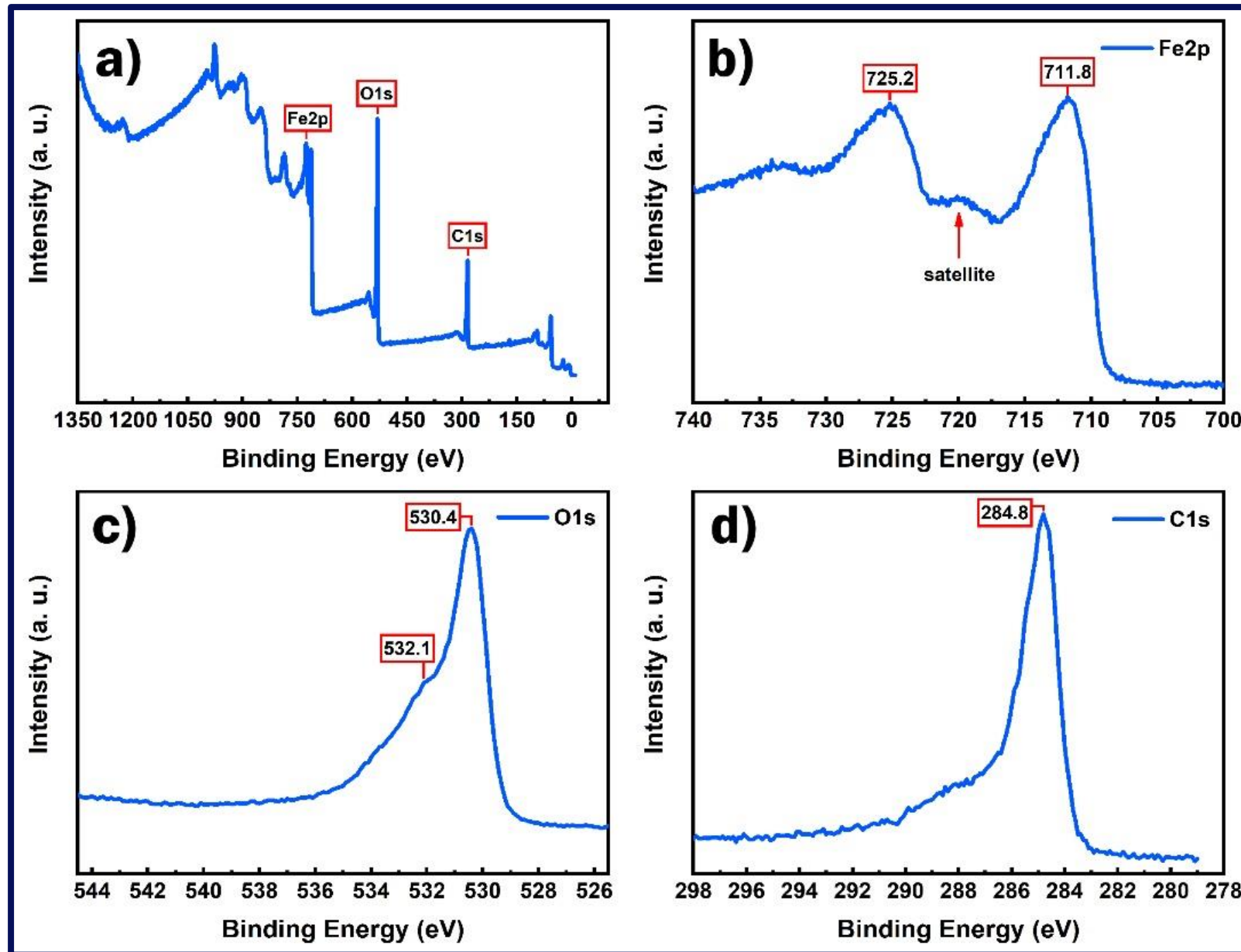


Figure 6. XPS survey spectrum (a), high-resolution XPS spectra of Fe2p (b), O1s (c), and C1s (d) for the Fe₂O₃/MWCNTs material

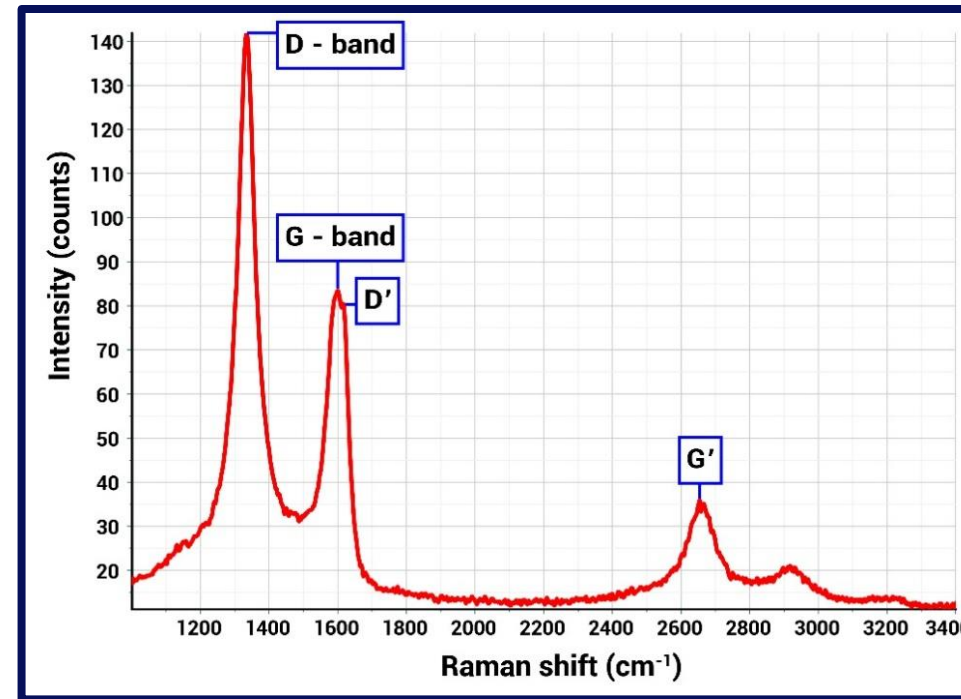


Figure 7. Raman spectrum of the MWCNTs structure material

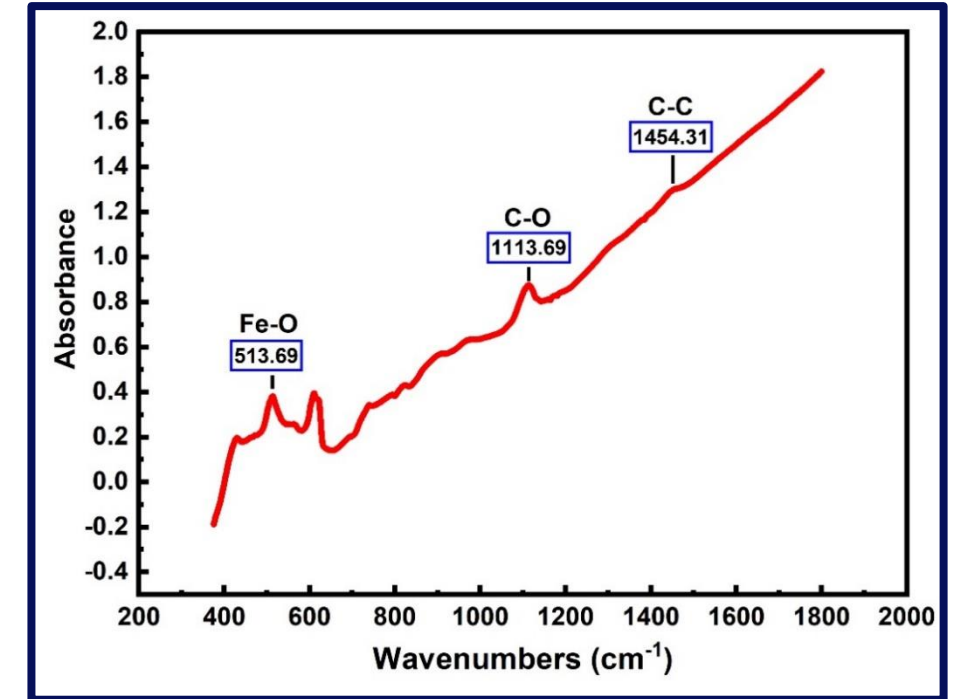


Figure 8. FTIR spectrum of the Fe₂O₃/MWCNTs material

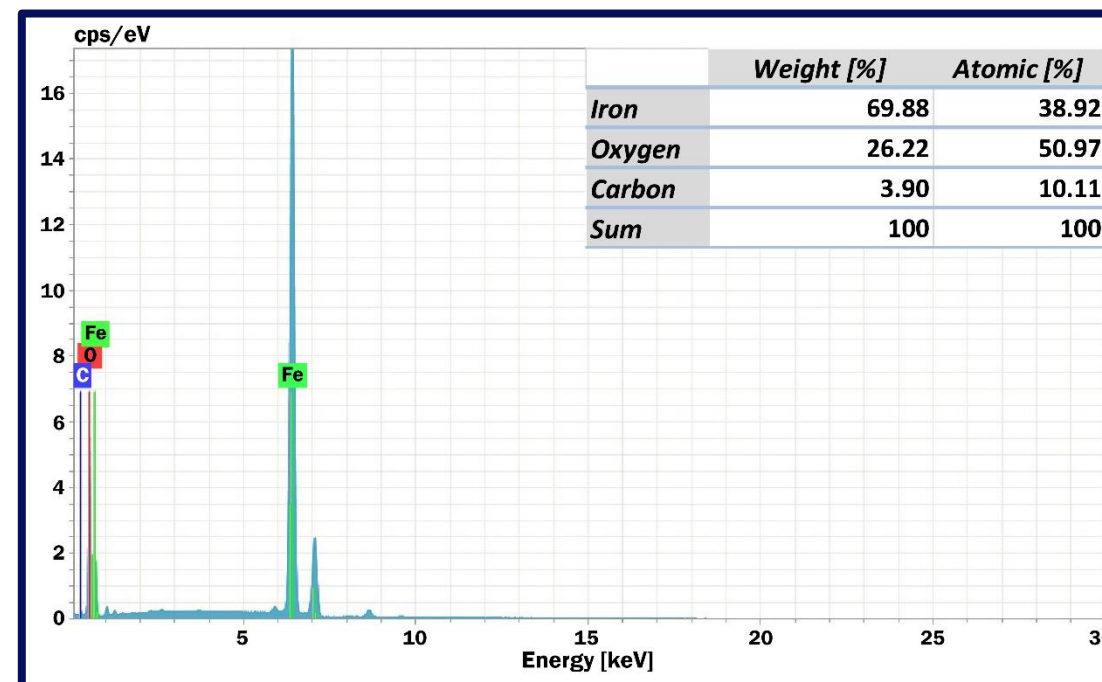


Figure 9. EDX spectrum of the Fe₂O₃/MWCNTs material

Raman analysis showed D, G, and G' bands at 1340, 1600, and 1616 cm⁻¹, respectively, with an I(D)/I(G) ratio of 1.701 ± 0.02, confirming defect-rich MWCNTs. FTIR spectra revealed characteristic peaks at 513.69, 628, and 1454.31 cm⁻¹, verifying Fe₂O₃/MWCNTs formation and surface modification. XPS detected Fe2p peaks at 711.8 and 725.2 eV, while EDX analysis showed 3.9 wt.% carbon and 26.22 wt.% oxygen.

Results

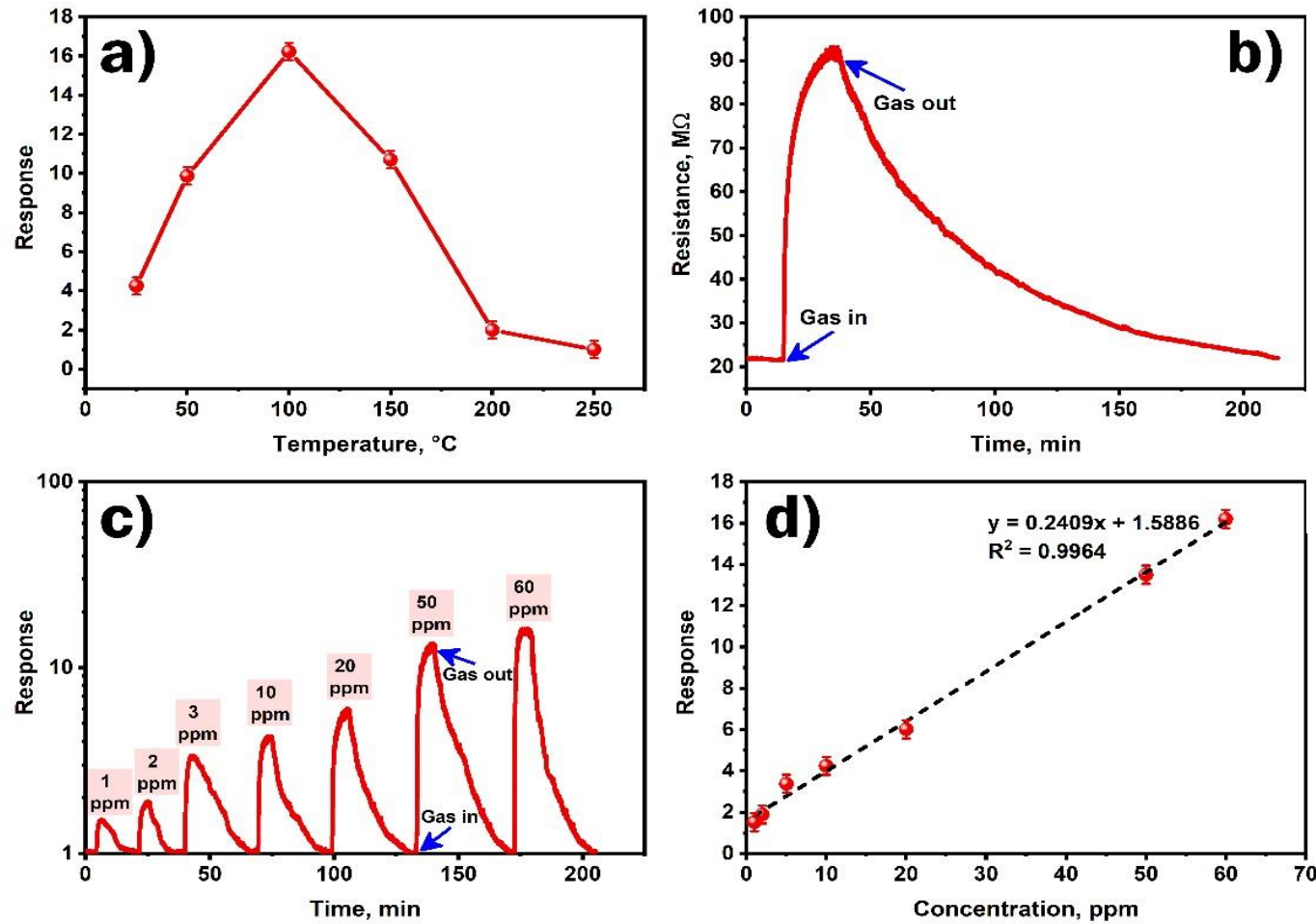


Figure 10. (a) Sensor response vs. operating temperature at 60 ppm HPV, (b) dynamic resistance curve under the influence of 60 ppm of HPV at room temperature, (c) dynamic response curves at different concentrations of HPV at 100 °C (d) sensor response vs. HPV concentration at 100 °C.

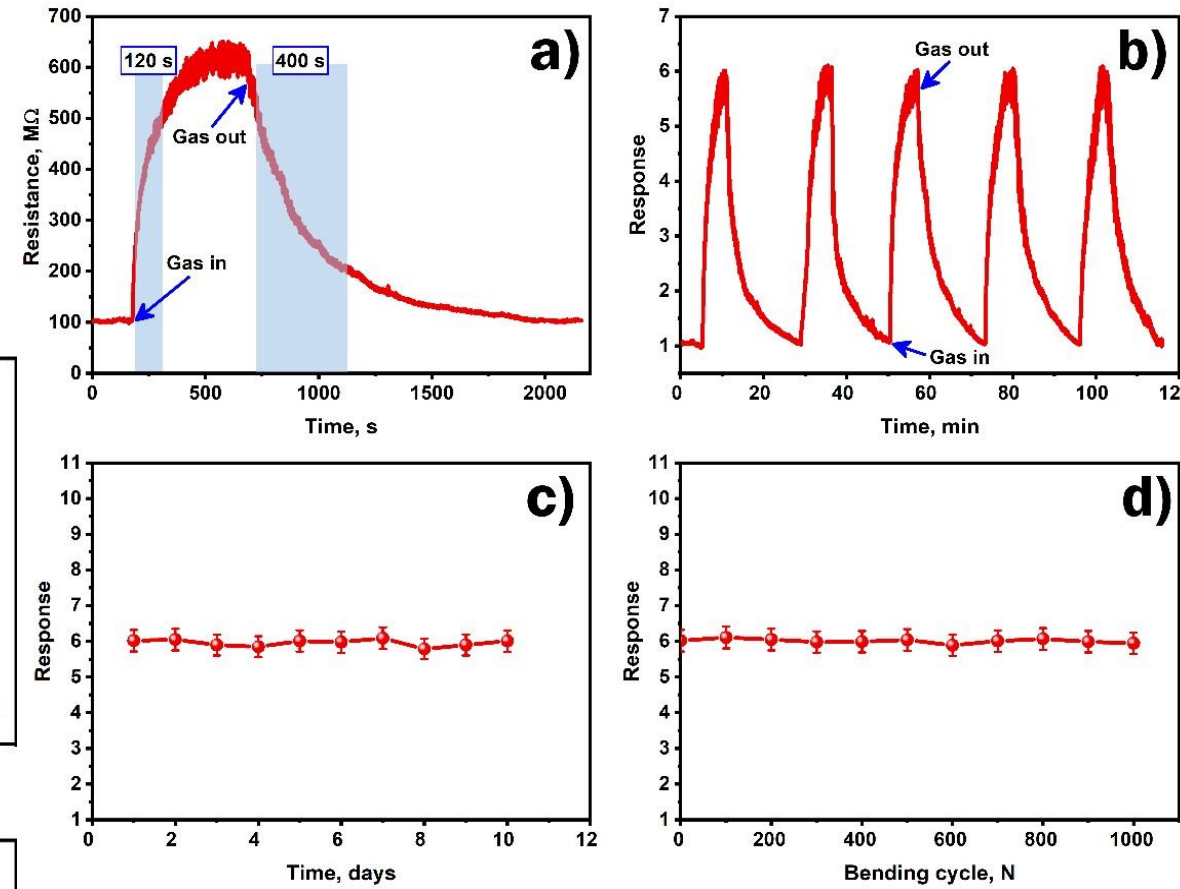


Figure 11. (a) Real-time resistance curve of the sensor at 20 ppm HPV, representing the response and recovery times at 100 °C, (b) repeatability tests of the sensor to 20 ppm HPV at 100 °C, (c) long-term stability of the HPV sensor at 100 °C, (d) bending stability of the HPV sensor at 100 °C.

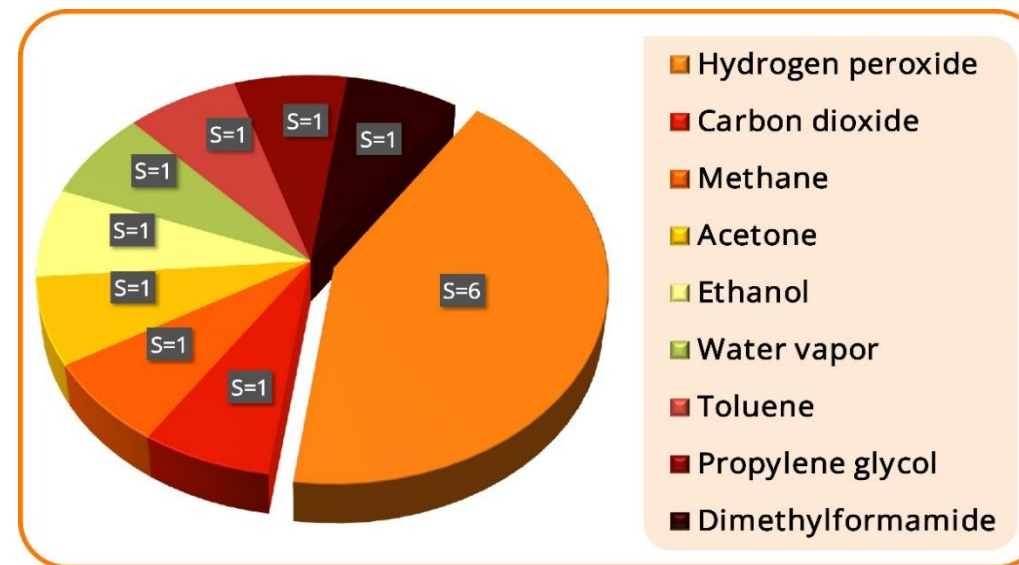
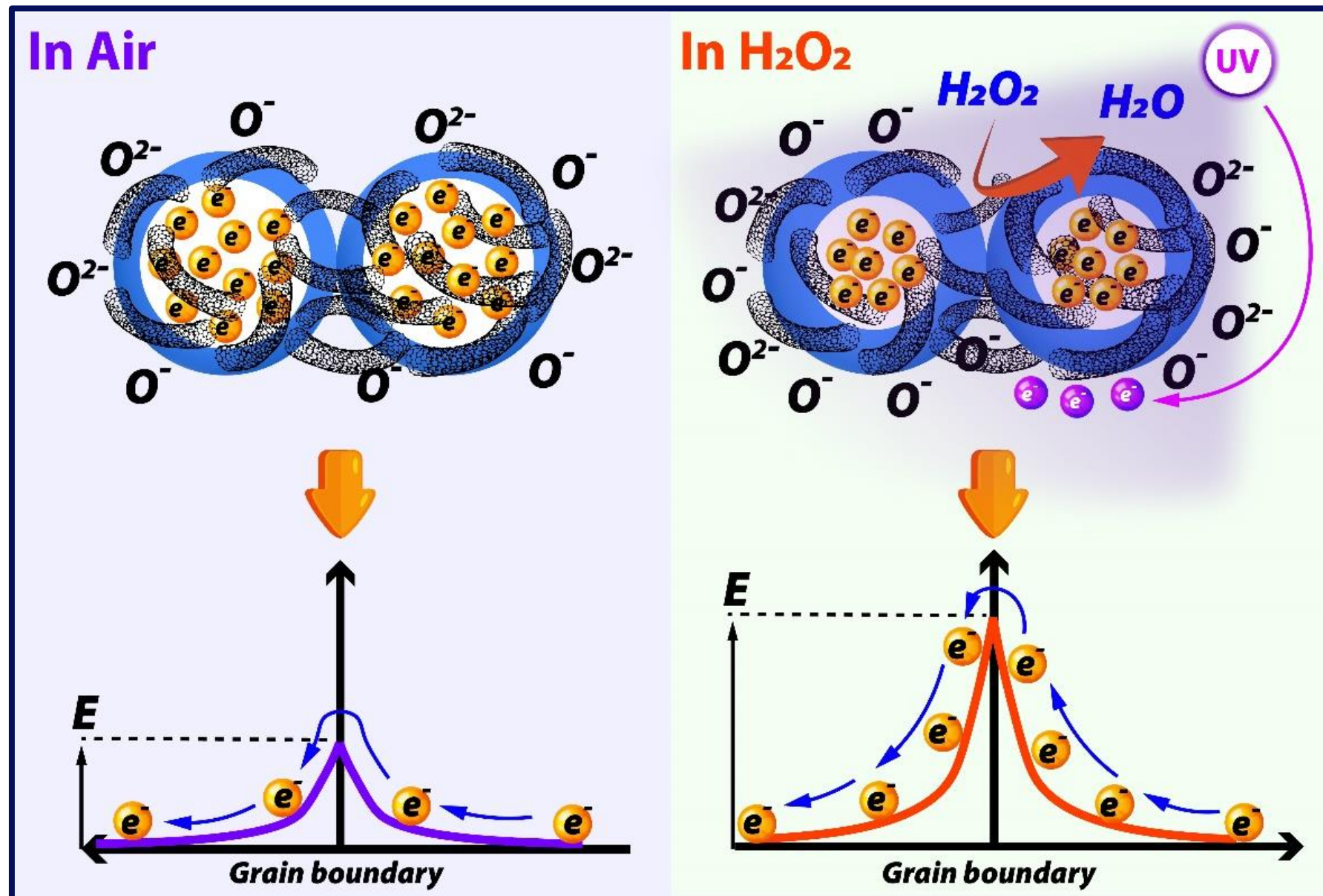


Figure 12. Selectivity of the sensor for 20 ppm of HPV at 100 °C.

The Fe₂O₃/MWCNTs sensor exhibited the highest response of 16.23 to 60 ppm HPV at an optimal operating temperature of 100°C, while at room temperature the resistance increased from 22 to 93 MΩ within 12 min. The sensor detected HPV concentrations as low as 1 ppm with a response of 1.52 and showed a linear response toward increasing HPV concentration. At 20 ppm HPV, the resistance increased about 6 times, with a response time of 120 s and recovery time of ~400 s. The sensor demonstrated excellent repeatability, long-term stability over 10 days with a maximum deviation of 2.85%, and maintained an average response of 6.01 after 1000 bending cycles with only 0.74% error. The Fe₂O₃/MWCNTs structure also showed outstanding selectivity toward HPV without response to interfering gases or humidity changes.

HPV sensing mechanism



Conclusion

This work demonstrated the synthesis of a novel HPV-sensitive Fe₂O₃/MWCNTs flexible nanocomposite with enhanced sensing performance fabricated by RF/DC sputtering. SEM and TEM analyses revealed Fe₂O₃ grain sizes of 25–40 nm and MWCNT diameters of 10–20 nm with lengths of tens of micrometers, while Raman, XPS, and FTIR analyses confirmed the chemical composition and structural characteristics of the material. The sensor exhibited HPV sensing capability even at room temperature, where its resistance increased about 4 times, while the optimal operating temperature was 100°C with a low detection limit of 1 ppm ($S = 1.52$). The response and recovery times were 120 and 400 s, respectively, and the sensor showed a linear response toward HPV concentration together with excellent long-term, mechanical, and selective stability. These results demonstrate the strong potential of the Fe₂O₃/MWCNTs nanocomposite for next-generation HPV sensing applications.



Center/Chair of
Materials Science
& Nanotechnologies

Առաջընթաց՝ արդյունավետ գիտությամբ «ԱԱԳ-2026»

ՄԵՆՍՈՐԱՅԻՆ ՀԱՄԱԿԱՐԳԵՐԻ ՆԱԽԱԳԾՈՒՄ
Ե ՊԱՏՐԱՍՏՈՒՄ ՆԱՆՈԿԱՌՈՒՑՎԱԾՔԱՅԻՆ
ՆՅՈՒԹԵՐԻ ՀԻՄԱՆ ՎՐԱ

*This research was funded by the Higher Education and Science
Committee of MESCS RA (Research project N° 24LCG- 2J001)*

Thank You

Rima Papovyan



rimapapovyan@ysu.am,
maleksanyan@ysu.am,
nanotech@ysu.am

